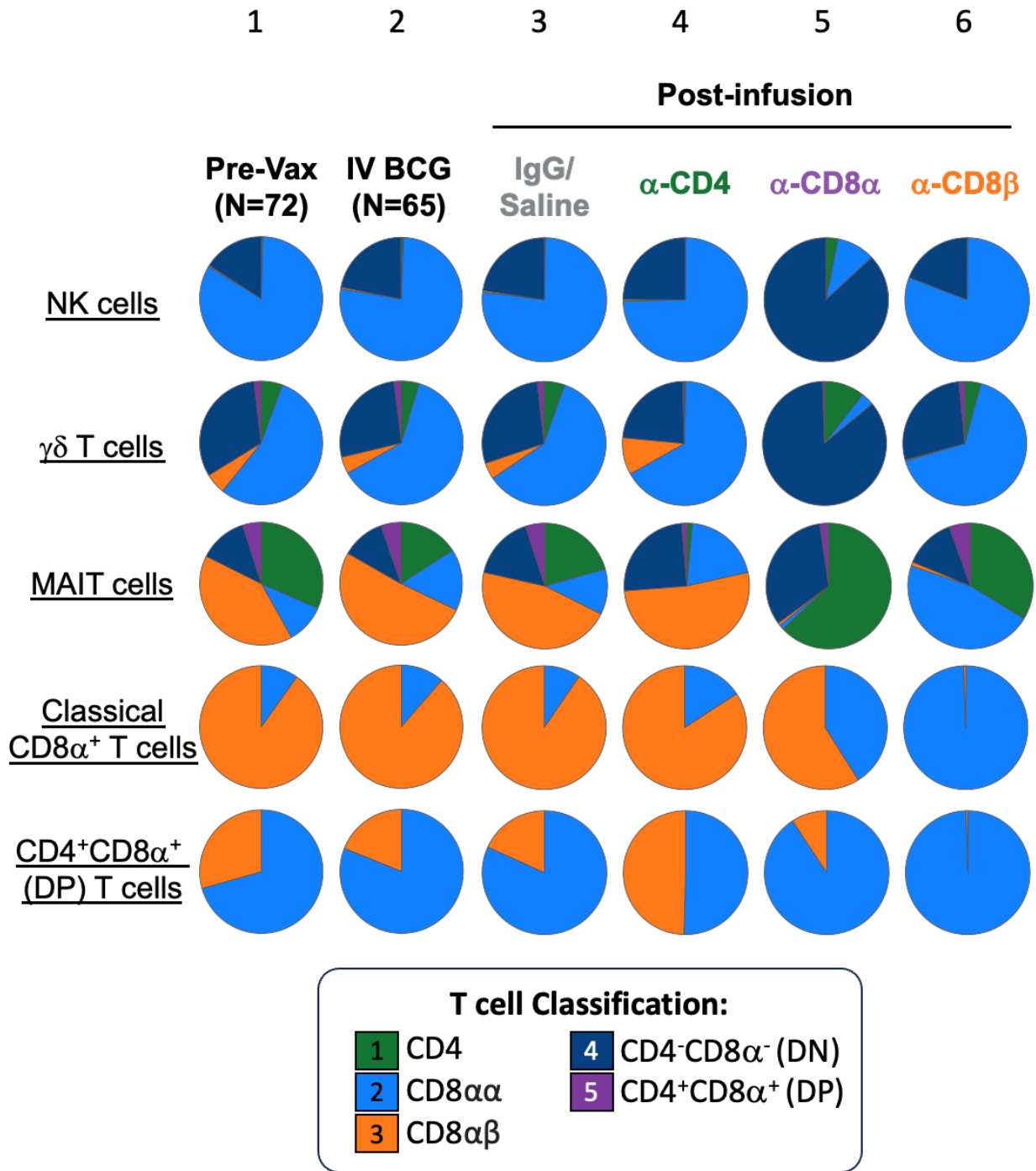


- 1 **Supplementary Materials for**
- 2 **CD4 T cells and CD8 α + lymphocytes are necessary for intravenous BCG-induced protection**
- 3 **against tuberculosis in macaques**
- 4

5 Fig. S1



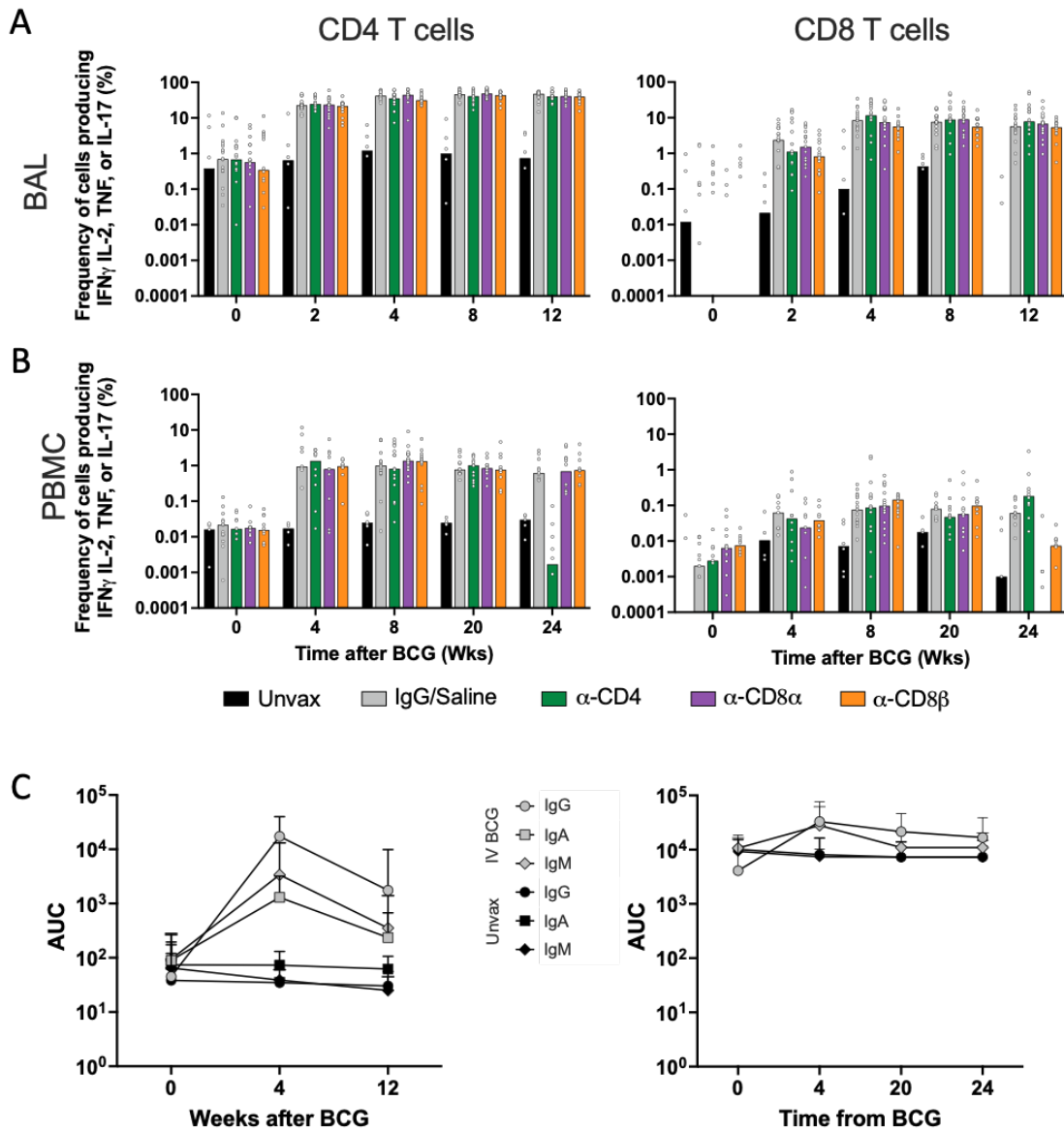
6

7 **Supplemental Figure S1. Changes in the composition of lymphocyte cell types in blood of IV**

8 **BCG vaccinated macaques following cell type depletion.** Frequency of common lymphocyte

9 cell types' CD4 and CD8α/β distributions measured by flow cytometry. CD4 (green), CD8αα

10 (light blue), CD8 $\alpha\beta$ (orange), CD4-CD8- (dark blue), and CD4+CD8+ (purple) phenotypes are
11 shown for each cell type. NK cells (top row), $\gamma\delta$ T cells (second row), MAIT cells (third row),
12 Classical CD8+ T cells (fourth row), and CD4+CD8+ T cells (bottom row) are shown. Columns
13 show baseline (1), following vaccination (2), and the effects of each infusion (3-6).
14



16

17 **Supplemental Figure S2. Cellular and humoral responses to IV BCG peak four to eight**

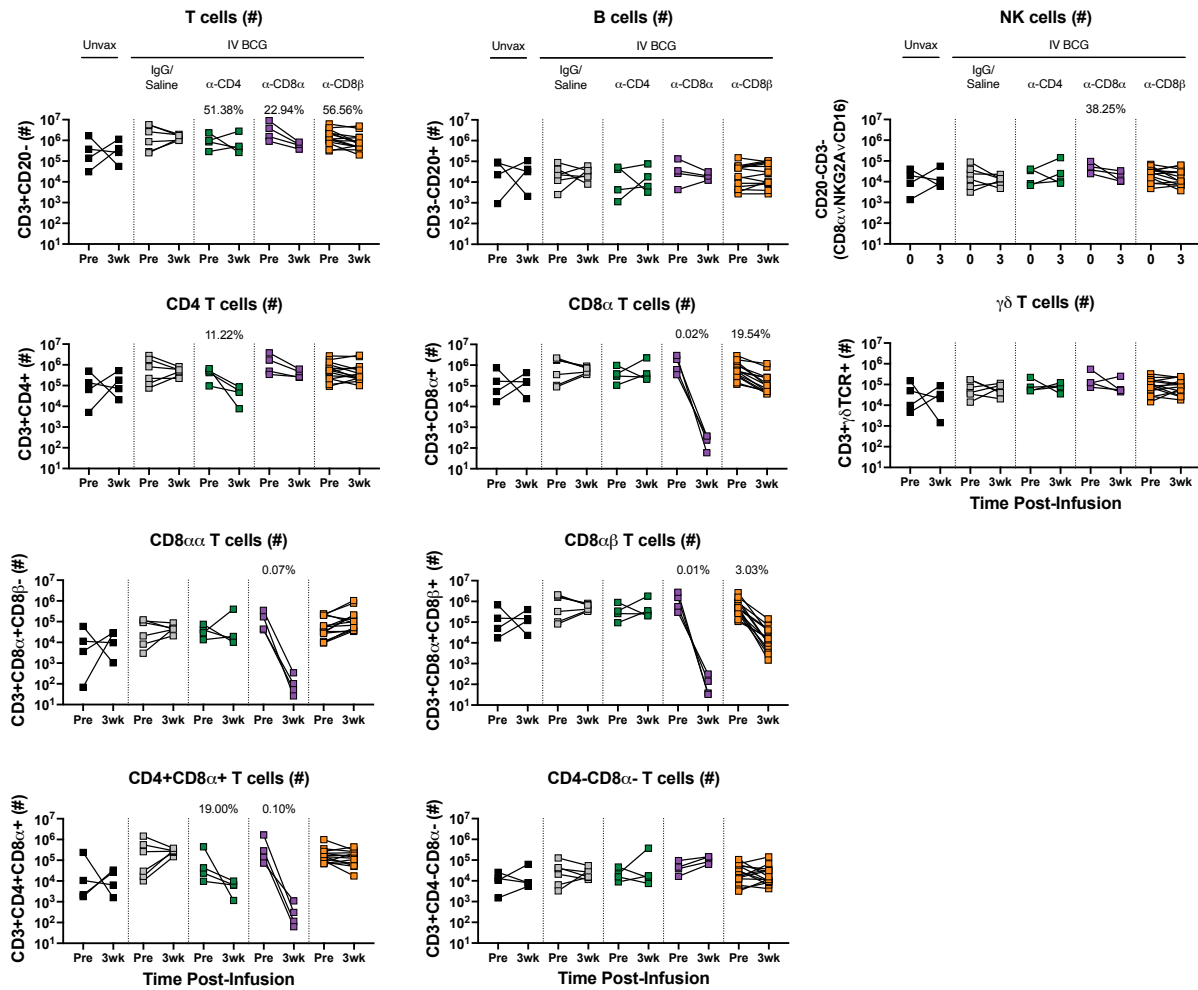
18 **weeks post-vaccination. (A,B) Frequency of cytokine (IFN γ , TNF, IL-2, and/or IL-17) producing**

19 **CD3+CD4+ (left) and CD3+CD8 α + (right) T cells in BAL (A) and PBMCs (B) in response to**

20 **WCL stimulation. (C) Antibody titers to mycobacterial antigens in concentrated BAL fluid (left)**

21 **and plasma (right).**

22



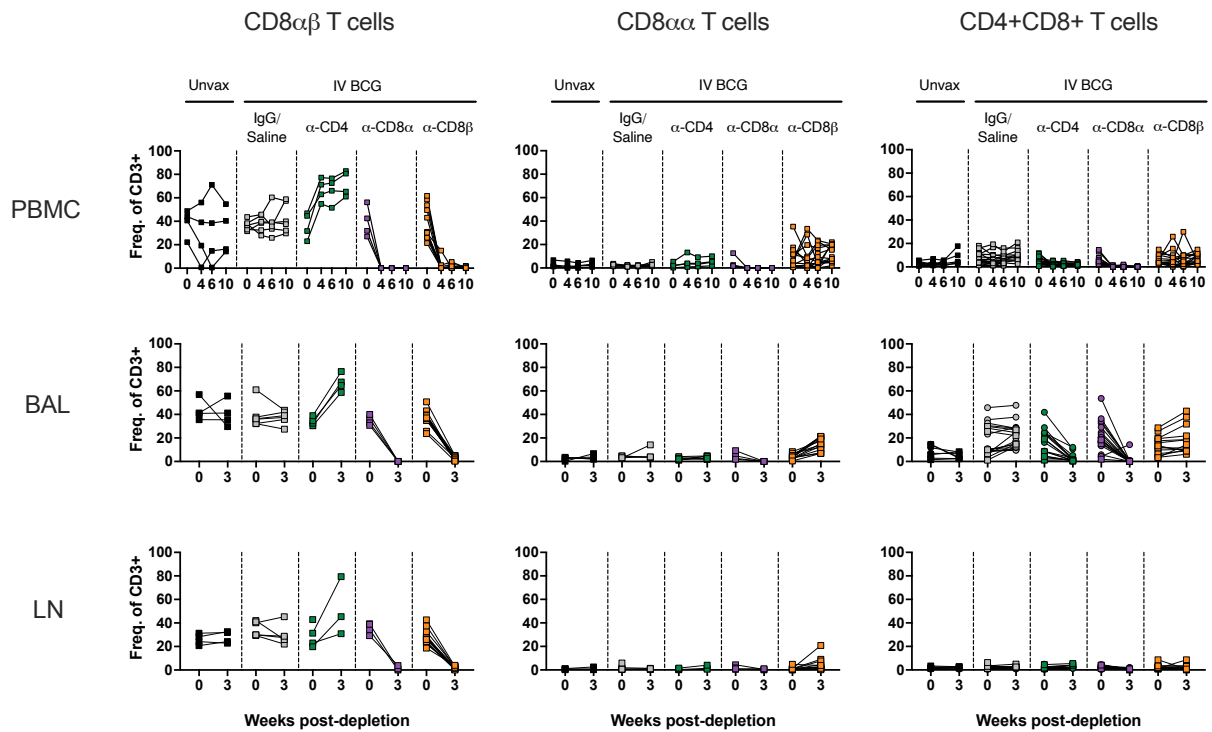
24

25 **Supplemental Figure S3. Targeted lymphocyte subsets were successfully depleted in BAL.**

26 Numbers of all lymphocyte subsets pre- and post-depletion in BAL were characterized by flow
 27 cytometry. Only animals in the second cohort are included, as anti-CD20 and anti-CD8β antibodies
 28 were not included in the flow cytometry panels for the first cohort. Percentages shown in each plot
 29 represent population size relative to pre-depletion samples, calculated by group median.

30

31 **Fig. S4**



32

33 **Supplemental Figure S4. CD3+CD8+ T cell subsets are selectively depleted following CD8 α**

34 **and CD8 β depletion.** Left panels: Conventional CD8 $\alpha\beta$ T cells (CD20-CD3+ $\gamma\delta$ TCR-CD4-

35 CD8 α +CD8 β +); middle panels: unconventional CD8 $\alpha\alpha$ T cells (CD20-CD3+ $\gamma\delta$ TCR-CD4-

36 CD8 α +CD8 β -); right panels: CD4+CD8+ double positive T cells (CD20-CD3+ $\gamma\delta$ TCR-

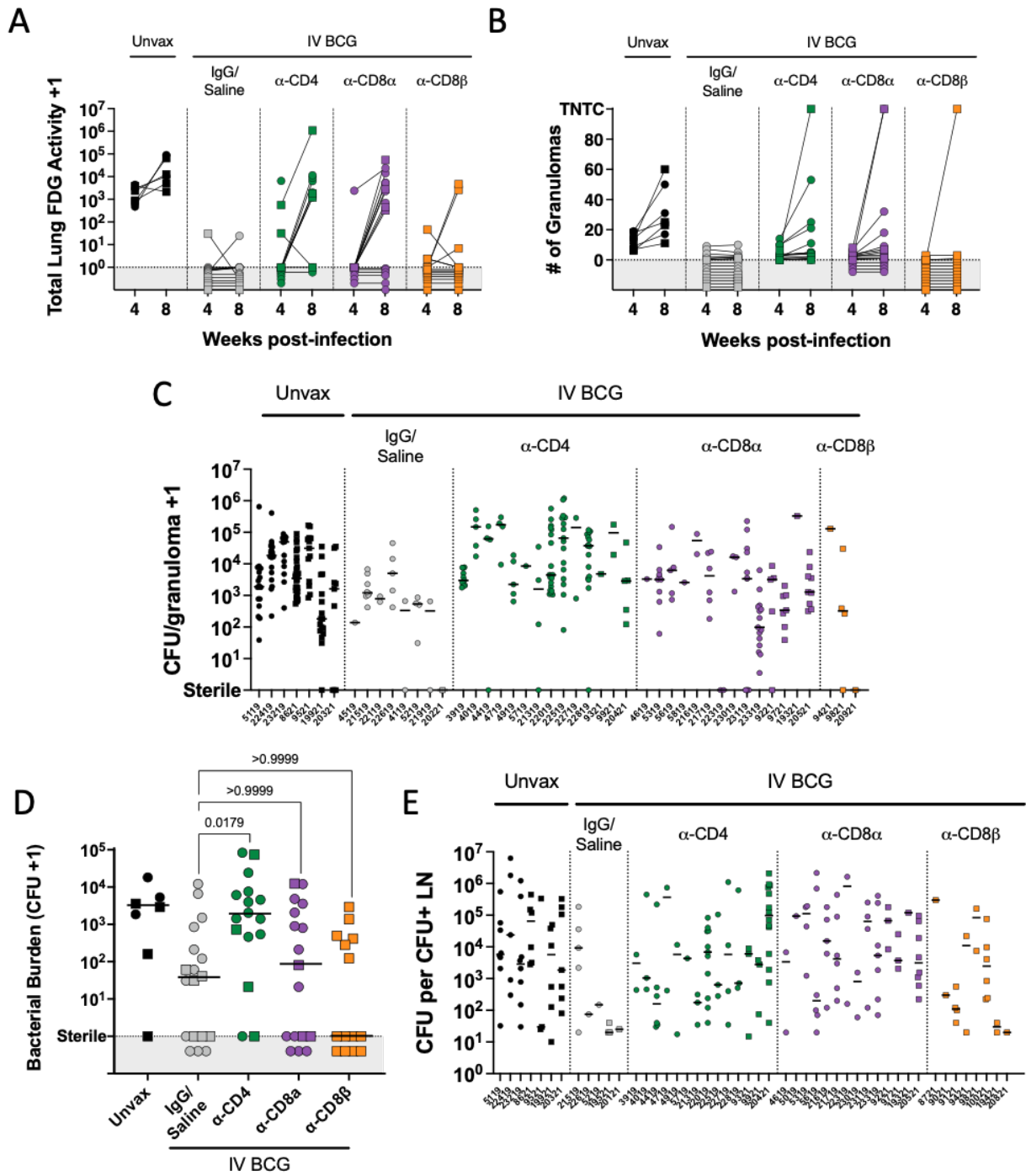
37 CD4+CD8 α +). Top panels: PBMC; middle panels: BAL; bottom panels: peripheral LNs.

38 Populations are reported as a frequency of CD3+ T cells. Only animals in the second cohort are

39 included, as a anti-CD8 β antibody was not included in the flow cytometry panels for the first

40 cohort.

41



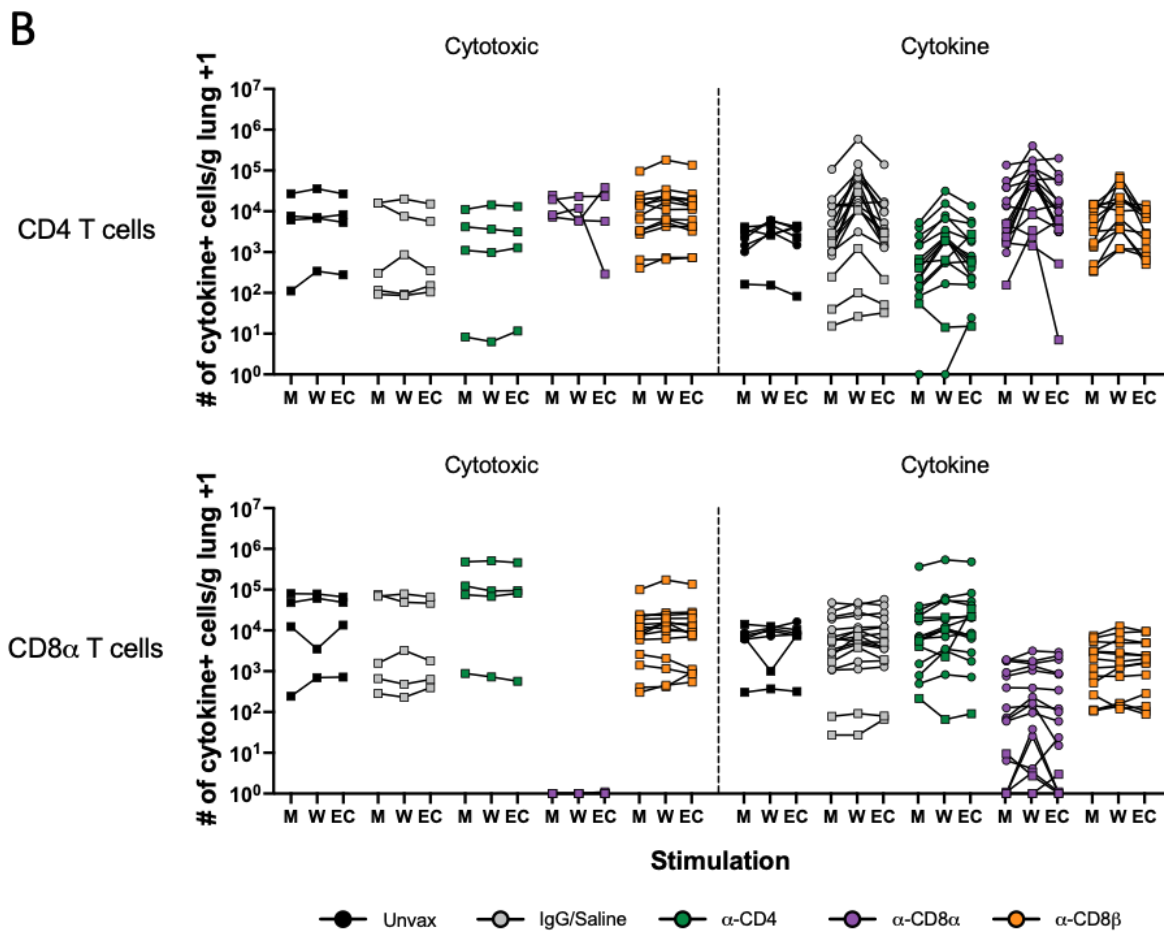
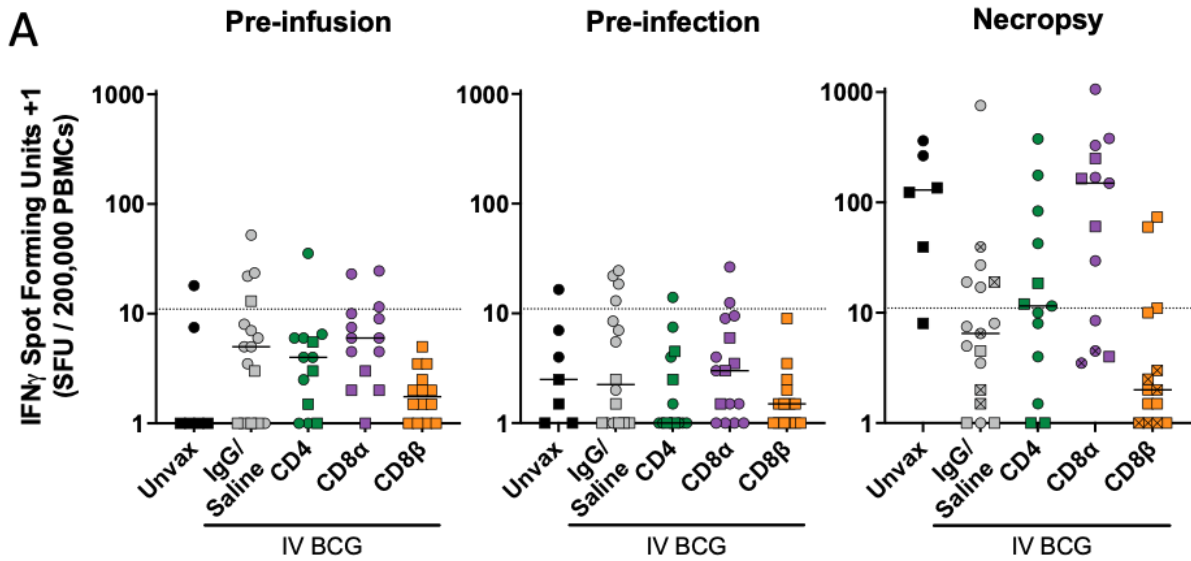
43

44 Supplemental Figure S5. CD4 and CD8α depletion lead to increased disease and bacterial

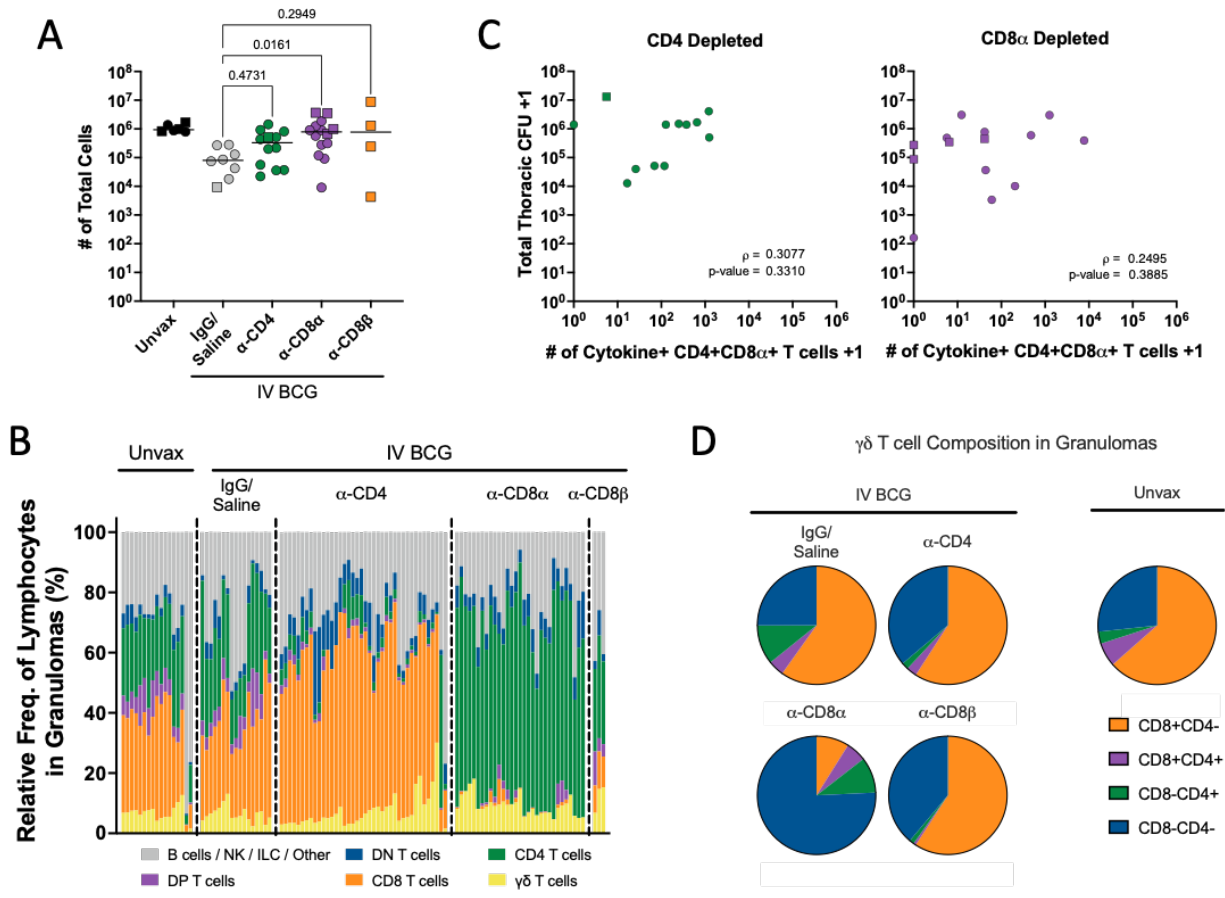
45 burden. (A) Total lung FDG activity at 4 and 8 weeks post-Mtb challenge. Animals with missing

46 PET scans were not included. Unvax: n = 7 (4wk), 6 (8wk); IgG/Saline: n = 16 (4wk & 8wk); α -
47 CD4: n = 15 (4wk), 11 (8wk); α -CD8 α : n = 16 (4wk & 8wk); α -CD8 β : n = 14 (4wk & 8wk). **(B)**
48 Number of granulomas seen by PET CT scans at 4 and 8 weeks post-infection. TB pneumonia or
49 consolidations are denoted as too numerous to count (TNTC). For panels A and B, each symbol
50 represents an animal, and lines connect animals across timepoints. **(C)** CFU per granuloma
51 separated by animal. **(D)** Bacterial burden in lung lobes without gross pathology (i.e. non-
52 granuloma tissue). Symbols represent an animal. Groups were compared using the Kruskal-Wallis
53 test, with Dunn's multiple comparison adjusted p-values shown, comparing IgG/Saline group
54 against each depletion group. Groups were compared using the Kruskal-Wallis test, with Dunn's
55 multiple comparison adjusted p-values shown, comparing IgG/Saline group against each depletion
56 group. **(E)** CFU of non-sterile thoracic LN separated by animal. In panels A, B, and D, symbols in
57 gray regions are of equal value (0 or sterile) and were spread for better visualization. In panels C
58 and E, each symbol represents a granuloma or LN, and each column represents an animal. Circles
59 represent cohort 1, squares represent cohort 2.

60



64 **are altered after depletion.** (A) Enzyme-linked immunospot (ELISpot) interferon gamma release
65 assay results following stimulation with ESAT6 and CFP10 peptide pools. Spot forming units
66 (SFU) were normalized to unstimulated background. A response of 10 SFU per 200,000 PBMCs
67 is considered positive for an Mtb-specific response (18). Pre-infusion: post-vaccination, pre-
68 depletion (Unvax: n = 6; IgG/Saline: n = 16; α -CD4: n = 13; α -CD8 α : n = 14; α -CD8 β : n = 14).
69 Pre-infection: post-depletion, pre-Mtb challenge (Unvax: n = 7; IgG/Saline: n = 16; α -CD4: n =
70 14; α -CD8 α : n = 16; α -CD8 β : n = 14). Necropsy: at necropsy (Unvax: n = 6; IgG/Saline: n = 17;
71 α -CD4: n = 13; α -CD8 α : n = 13; α -CD8 β : n = 14). Lines represent group median. Symbols with
72 a cross represent sterile animals. (B) Number of CD4 (*top*) and CD8 α + (*bottom*) T cells producing
73 cytotoxic molecules (GrzB/GrzK) or cytokines (IFN γ /TNF/IL-2/IL-17) stimulated with WCL (W)
74 or ESAT-6 and CFP10 peptide pools (EC) or without stimulation (media, M). Lines connect
75 animals. Symbols represent an animal, circles represent cohort 1 and squares represent cohort 2.
76



78

79 **Supplemental Figure S7. Granuloma lymphocyte composition.**

80 granuloma. Each symbol represents the mean of all granulomas in an animal, line represents the

81 group median. All groups (excluding the unvaccinated animals) were compared using the Kruskal-

82 Wallis test with Dunn's multiple comparison adjusted p-values reported, comparing IgG/Saline

83 group against each depletion group. **(B)** The relative frequencies of lymphocyte populations in

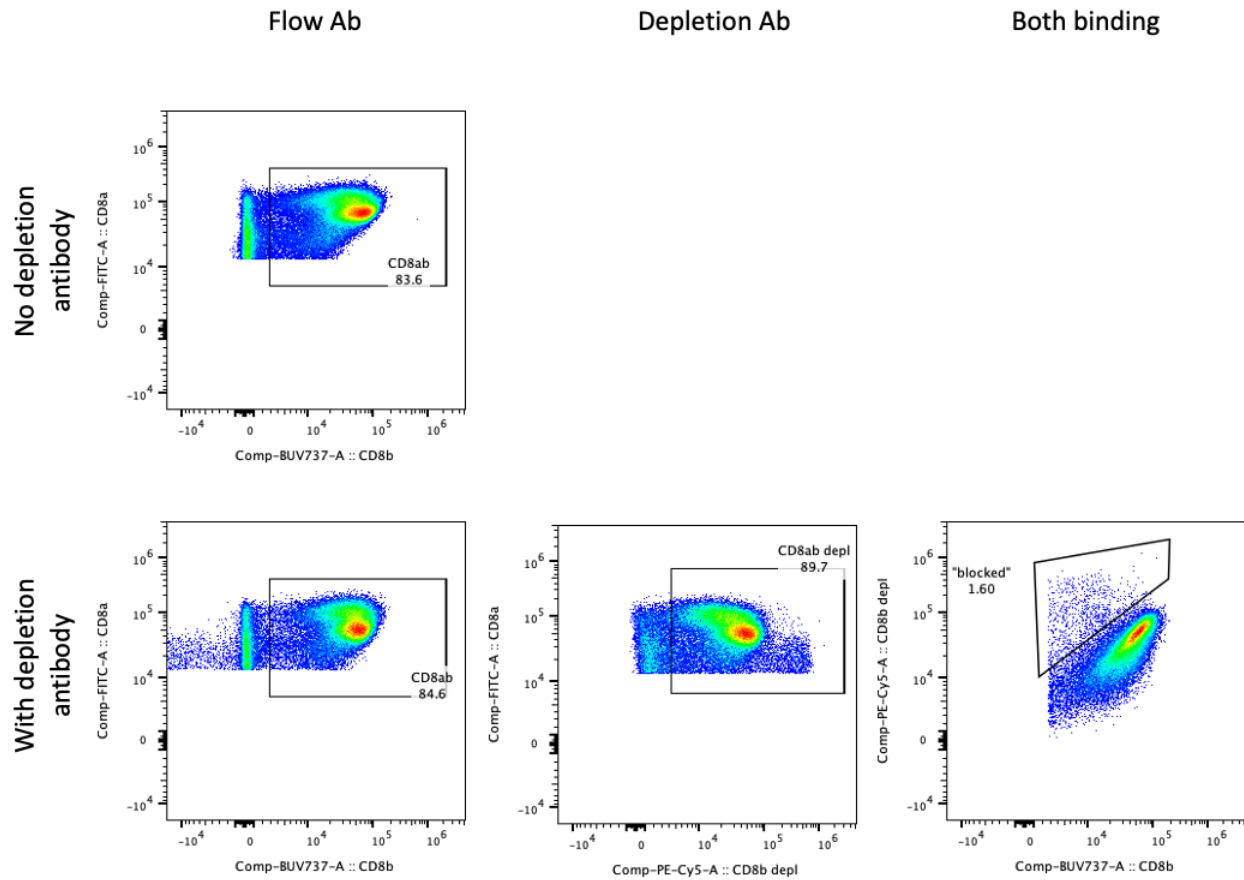
84 granulomas. Each bar represents a granuloma, divided by depletion group. B / NK / ILC / Other

85 are CD3- populations. **(C)** Relationship between CD4+CD8 α + double positive T cell numbers in

86 granulomas and bacterial burden (CFU). The number of CD4+CD8 α + T cells were determined for

87 all granulomas excised from CD4- (left) and CD8 α - (right) depleted animals. Symbols shown

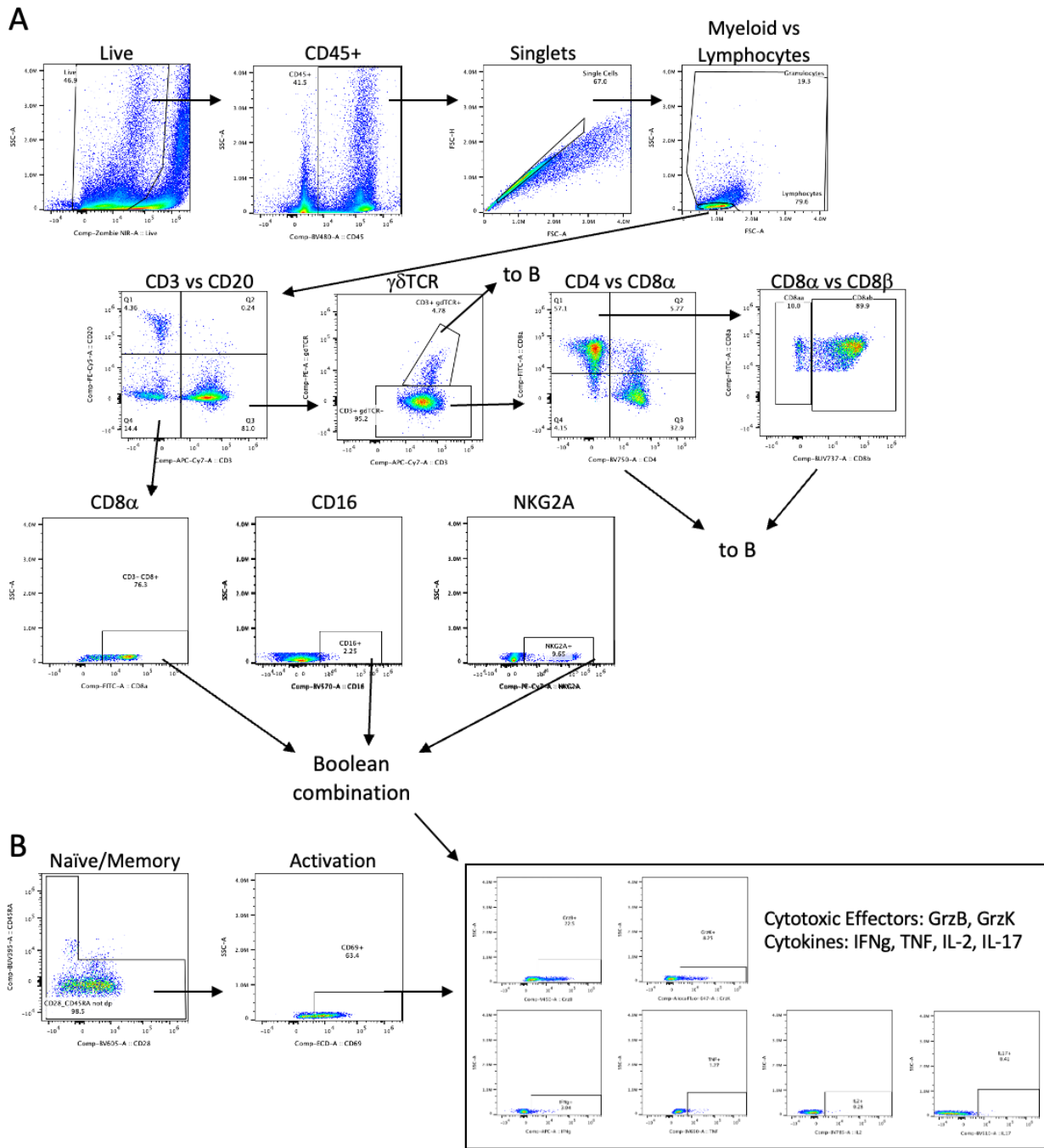
88 represent mean per animal plotted against total thoracic CFU for the animal. Spearman correlation
89 coefficient (ρ) and p-value shown. In panels A and C, circles represent cohort 1 and squares
90 represent cohort 2. **(D)** Relative abundance of CD4⁺ and/or CD8 α ⁺ $\gamma\delta$ T cells found in
91 granulomas.
92



94

95 **Supplemental Figure S8. CD8 β staining by flow cytometry is not inhibited by anti-CD8 β**
 96 **depletion antibody.** PBMCs stained with or without the addition of the depletion a-CD8 β
 97 antibody show similar levels of staining by the antibody used for flow cytometry, indicating
 98 negligible competitive blocking.

99

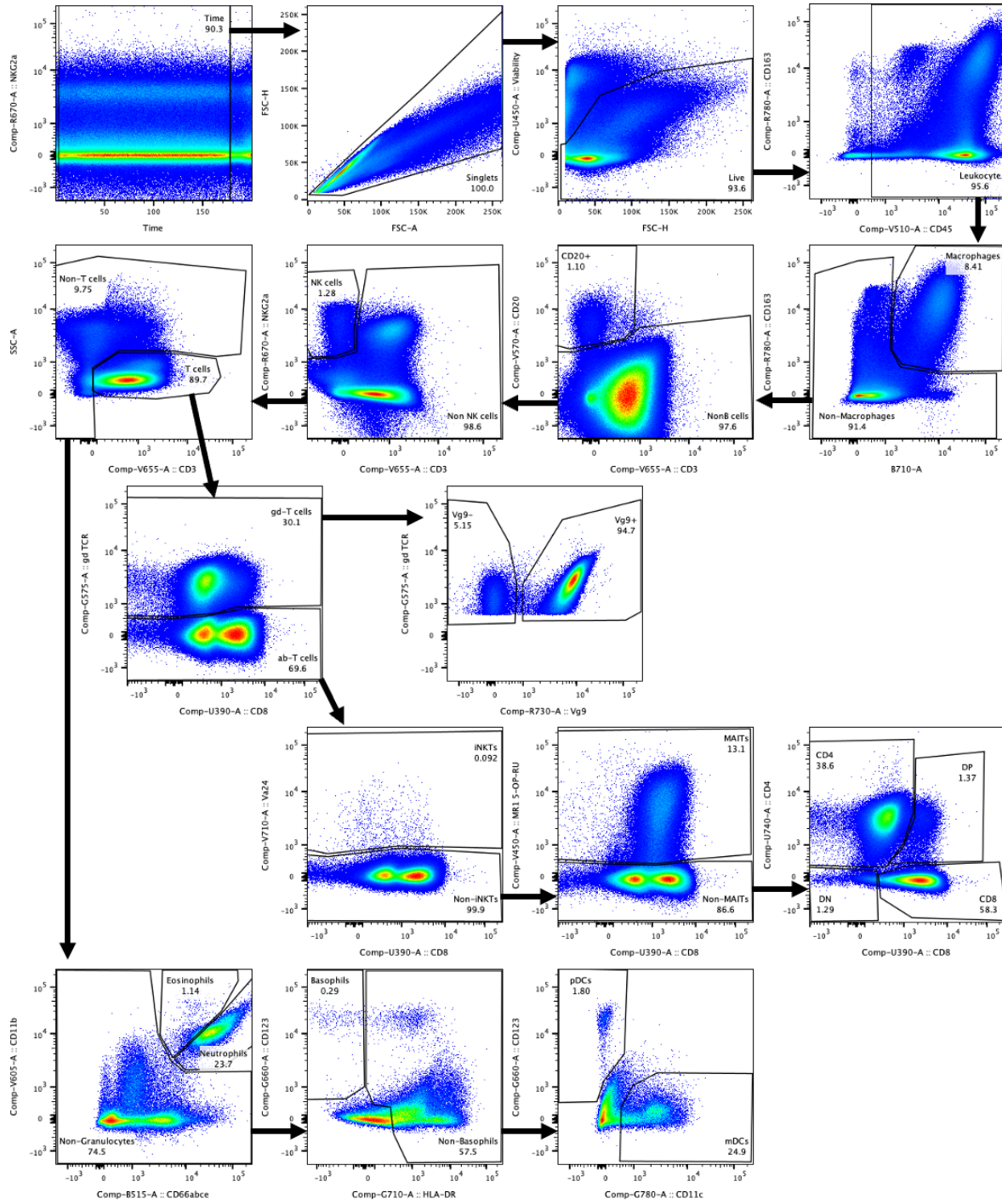


101

102 **Supplemental Figure S9. Gating strategy for flow cytometry samples. Representative lung**

103 tissue from a vaccinated, undepleted animal.

104



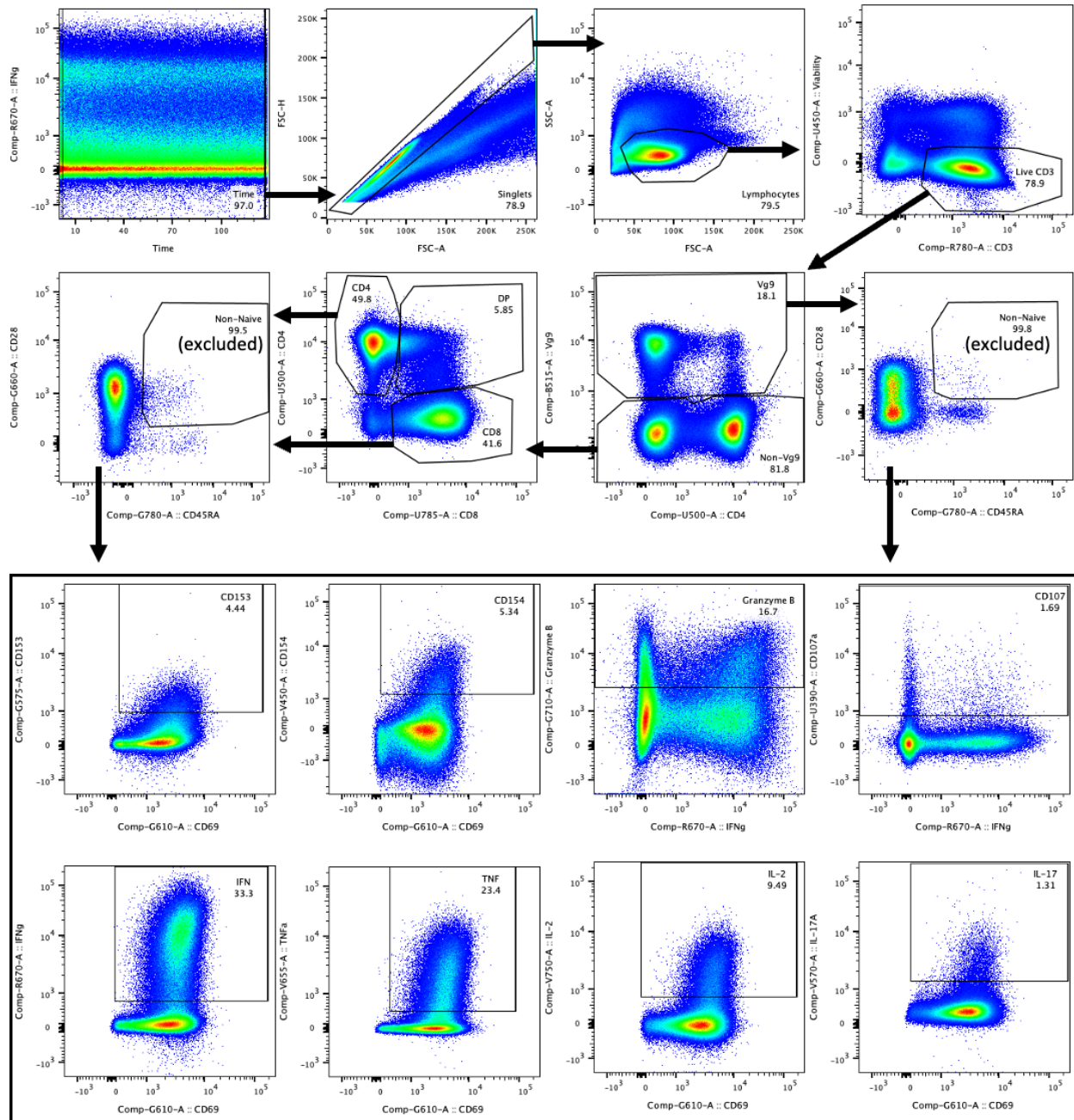
106

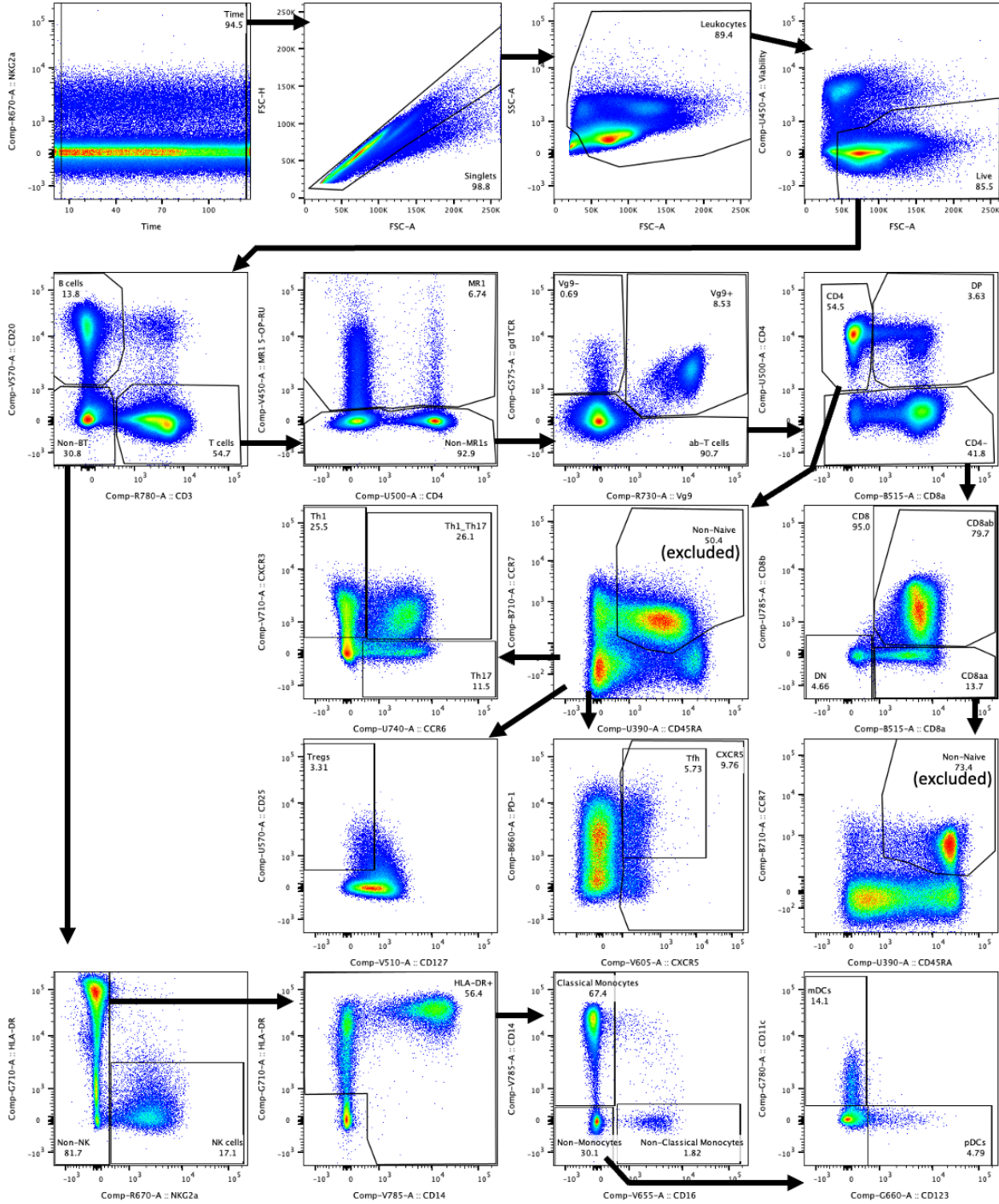
107 Supplemental Figure S10. Gating strategy for BAL phenotyping flow cytometry samples.

108 Representative BAL sample from an IV BCG-vaccinated animal at a peak timepoint.

109

110 Fig. S11





117

118 **Supplemental Figure S12. Gating strategy for PBMC phenotyping flow cytometry samples.**

119 Representative PBMC sample from an IV BCG-vaccinated animal at a peak timepoint.

120

121 **Supplemental Table S1. NHP vaccination, depletion, infection and outcomes.** A glossary with
122 additional definitions is included on the second sheet.

123

124 **Supplemental Table S2. Antibodies used for spectral flow cytometry.** Each sheet contains
125 details about antibodies used to collect flow cytometry data in the listed figures.

126

127 **Data file S1. Relative abundance of detected barcodes in CFU+ tissues.** Each sheet contains
128 data from all animals in a depletion group.

129